Chinese Herbal Medicines 13 (2021) 342–350

Contents lists available at ScienceDirect

Chinese Herbal Medicines

journal homepage: www.elsevier.com/locate/chmed

Original Article

Investigating pharmacological mechanisms of andrographolide on non-alcoholic steatohepatitis (NASH): A bioinformatics approach of network pharmacology

Lei Li [a,b], Sheng-he Li [a], Jin-peng Jiang [a], Chang Liu [a,*], Li-li Ji [b,*]

[a] Key Laboratory of Quality & Safety Control for Pork, Ministry of Agriculture and Rural, Anhui Key Laboratory of Animal Nutritional Regulation and Health, College of Animal Science, Anhui Science and Technology University, Fengyang 233100, China
[b] Shanghai Key Laboratory of Compound Chinese Medicines, MOE Key Laboratory for Standardization of Chinese Medicines, Institute of Chinese Materia Medica, Shanghai University of Traditional Chinese Medicine, Shanghai 201203, China

ARTICLE INFO

Article history:
Received 3 June 2020
Revised 19 August 2020
Accepted 25 October 2020
Available online 13 May 2021

Keywords:
andrographolide
network pharmacology
non-alcoholic steatohepatitis
molecular docking

ABSTRACT

Objective: To investigate the mechanisms of andrographolide against non-alcoholic steatohepatitis (NASH) based on network pharmacology, so as to provide a reference for further study of andrographolide in the treatment of NASH and other metabolic diseases.
Methods: The methionine- and choline-deficient (MCD) diet-induced NASH mice were treated by administration of andrographolide, and serum transaminase and pathological changes were analyzed. The network pharmacology-based bioinformatic strategy was then used to search the potential targets, construct protein–protein interaction (PPI) network, analyze gene ontology (GO) and Kyoto encyclopedia of genes and genomes (KEGG) pathway enrichment, and conduct molecular docking to explore the molecular mechanisms.
Results: The predicted core targets TNF, MAPK8, IL6, IL1B and AKT1 were enriched in non-alcoholic fatty liver disease (NAFLD) signaling pathway and against NASH by regulation of *de novo* fatty acids synthesis, anti-inflammation and anti-oxidation.
Conclusion: This work provides a scientific basis for further demonstration of the anti-NASH mechanisms of andrographolide.

1. Introduction

Non-alcoholic fatty liver disease (NAFLD) is characterized by excessive fat accumulation in the liver. With the improvement of living standards and the changes of life style, the prevalence of NAFLD is increasing rapidly, which has become a public health problem in worldwide (Wruck et al., 2017; Qian et al., 2020). In western developed countries, the incidence of NAFLD in adults is about 20%−30% (Bedogni et al., 2014; Vernon et al., 2011). The incidence of NAFLD in China is growing from 17% (2003) to 22.4% (2012), and approximately 173–310 million of people were estimated to suffer from NAFLD (Xiao et al., 2019; Zhou et al., 2007). NAFLD has gradually become one of the most important factors leading to chronic liver disease in China, especially for adolescents. There are two phenotypes of NAFLD, the first is non-alcoholic fatty liver (NAFL) with isolated steatosis as the hallmark, and non-alcoholic steatohepatitis (NASH), the more aggressive subtype, is characterized by hepatocytes inflammatory injury and ballooning even progressing to fibrosis, cirrhosis and hepatocellular carcinoma (HCC) (Oseini & Sanyal, 2017). About 1/3 to 1/2 of NAFLD patients may develop NASH, and the incidence of liver cirrhosis within 10 years is 15%−25%, of which 30%−40% will be mortal for liver failure or HCC (Fazel et al., 2016; Rocha et al., 2019; Rosmorduc & Fartoux, 2012). The more serious situation is that NASH is usually associated with type 2 diabetes mellitus, cardiovascular and cerebrovascular diseases (Rocha et al., 2019), which poses a serious threat to human health and social development.

Andrographis paniculata (Burm.F.) Nees, a widely used traditional Chinese medicine (TCM), has the effects of antipyretic and detoxification, cooling blood and detumescence, and its ingredients are mainly diterpenoids and flavonoids (Hossain et al., 2014). Andrographolide, as a diterpene lactone, is one of the well-known ingredients of *A. paniculate*. Previous studies demonstrated that andrographolide has multiple pharmacological effects, such as anti-inflammation, immunomodulation, anti-viral,

* Corresponding authors.
E-mail addresses: liuc@ahstu.edu.cn (C. Liu), jilili@shutcm.edu.cn (L.-l. Ji).

https://doi.org/10.1016/j.chmed.2021.05.001
1674-6384/

anti-tumor, treatment of diabetes, hypotension, inhibition of platelet aggregation and anti-thrombosis and etc (Ji et al., 2007, 2016; Thakur et al., 2016; Wintachai et al., 2015; Yu et al., 2015). Moreover, andrographolide is also widely used as a hepatoprotective drug in some Asian countries. It was found that andrographolide could ameliorate alcohol-induced hepatocyte injury in mice (Singha et al., 2007), and andrographolide could activate nuclear factor erythroid 2-related factor 2 (Nrf2) signaling pathway to protect hepatocyte from H_2O_2, CCl_4 or arsenic-induced liver injury (Chen et al., 2014; Das et al., 2015; Mittal et al., 2016). Furthermore, andrographolide could inhibit the transcriptional activity of sterol regulatory element-binding proteins (SREBPs) to reduce the concentration of blood lipid and increase the sensitivity to insulin in high fat diet-induced obese mice (Ding et al., 2014). Although andrographolide plays a critical role in protecting liver and regulating lipid metabolism, there are few reports about the therapeutic effect of andrographolide on NASH. Therefore, the present study explored the amelioration of andrographolide on methionine-and choline-deficient (MCD) diet-induced NASH mice and revealed the mechanisms of andrographolide in treatment of NASH based on network pharmacology, which may provide a theoretical basis for clinical application.

2. Material and methods

2.1. Chemical compounds and reagents

Andrographolide (purity greater than 98%) was purchased from Shanghai Macklin Biochemical Technology Co., Ltd (Shanghai, China). Pioglitazone was purchased from Wanbang Biochemical Pharmaceutical Group Co., Ltd (Jiangsu, China). Methionine-and choline-deficient (MCD) diet and methionine-choline supplemented (MCS) diet were purchased from Trophic Animal Feed High-tech Co. Ltd (Nantong, China). Kits of alanine aminotransferase (ALT) and aspartate aminotransferase (AST) were purchased from Nanjing Jiancheng Bioengineering Institute (Nanjing, China). Other reagents were obtained from Sigma Chemical Co. (St. Louis, MO, USA).

2.2. Animals and treatments

Male C57BL/6J mice [body weight (20 ± 2) g] were purchased from Qinglongshan Animal Breeder (SCXK 2017–0001, Nanjing, China). All animals were housed in an environmentally controlled room at (22 ± 2) °C with a 12 h light/dark cycle, and were free access to food and water. All animals received humane care in line with the institutional animal care guidelines approved by the Experimental Animal Ethical Committee, Anhui Science and Technology University. After one week of acclimation, 50 mice were divided into five groups (10 mice each) and fed with either the MCS diet or the MCD diet for four weeks: the Control (MCS diet), the NASH model (MCD diet), the positive control (MCD diet + pioglitazone 10 mg/kg), the low dose of andrographolide group (MCD diet + andrographolide 40 mg/kg) and the high dose of andrographolide group (MCD diet + andrographolide 80 mg/kg).

2.3. ALT/AST activity

The blood samples were kept at room temperature for 2 h, then samples were centrifuged at 1 500 × g for 15 min to collect the serum. Serum ALT/AST were measured with the kits according to the manufacturer's protocol.

2.4. Histological examination

The liver tissues were fixed in 10% phosphate buffered saline-formalin for at least 24 h. After dehydration with a sequence of ethanol solutions, the liver tissues were embedded in paraffin wax and sectioned at 5 μm thickness. At last, the sections were stained with hematoxylin and eosin (H&E) to evaluate liver injury.

2.5. Targets prediction of andrographolide

There are three ways to predict the targets for drugs, literature mining, chemical similarity searching and inverse docking (Zhao et al., 2019). To get comprehensive information about targets of andrographolide, DrugBank (https://www.drugbank.ca/) (Wishart et al., 2018), STITCH (http://stitch.embl.de/) (Szklarczyk et al., 2016), SwissTargetPrediction (http://www.swisstargetprediction.ch/) (Daina et al., 2019) and DRAR-CPI web servers (https://cpi.bio-x.cn/drar/) (Luo et al., 2011) were used to collect the targets of andrographolide. All the targets combined from each database were selected as the potential targets of andrographolide.

2.6. Collection of potential targets for NASH

"NASH" and "non-alcoholic steatohepatitis" were used as keywords to retrieve NASH associated targets in GeneCards database (https://www.genecards.org) (Stelzer et al., 2016) and Online Mendelian Inheritance in Man database (OMIM, https://omim.org) (Hamosh et al., 2005). On mapping NASH associated targets and predicted targets of andrographolide, we finally obtained the potential targets of andrographolide for treatment of NASH.

2.7. Construction and analysis of protein–protein interaction (PPI) network

The potential targets gene list was uploaded into STRING database (https://string-db.org, version 11.0) (Szklarczyk et al., 2018), with the species as "Homo sapiens" and a confidence score greater than 0.7, to obtain the data of PPI. Then, visualized PPI network was constructed with Cytoscape 3.6.0 software. Afterward, the topological parameters of the PPI network were analyzed with the Network Analyzer tool of Cytoscape. To obtain the key targets of the PPI network, the targets with greater than two times median of degree, and greater than the median of betweenness centrality (BC) and closeness centrality (CC) were selected (Miao et al., 2019).

2.8. GO and KEGG enrichment analysis

To assess the biological functions of the targets genes, Gene Ontology (GO) and Kyoto Encyclopedia of Genes and Genomes (KEGG) pathways enrichment analysis was performed using g:Profiler (https://biit.cs.ut.ee/gprofiler) (Raudvere et al., 2019) and visualized by the OmicShare tools, a free online platform (https://www.omicshare.com/tools) (Wang et al., 2019). Enriched GO terms and KEGG pathways with P-value $\leq$ 0.05 as a threshold were defined as significantly enriched terms and pathways comparing with the whole genome background.

2.9. Molecular docking analysis

To confirm the prediction of the core targets of andrographolide, molecular docking analysis was conducted by AutoDock 4.2 software (Morris et al., 2009). Briefly, the 3D structure file of the key targets were downloaded from RCSB PDB database (http://www.rcsb.org/) and the chemical structure file of andrographolide was obtained from PubChem (https://pubchem.ncbi.

nlm.nih.gov/), then both the proteins and andrographolide structure files were prepared by AutoDock Tools 1.5.6 software prior to performing the molecular docking process, including making energy minimize for andrographolide, and removing water molecules from proteins, adding hydrogen atoms, calculating and adding Gasteigar charges, merging non-polar hydrogen atoms and setting rotatable torsion bonds for protein molecules. Molecular docking was finally carried out by AutoDock 4.2 with the Lamarckian genetic algorithm and default parameters. The binding results were visualized and analyzed by PyMOL and ligplus software.

2.10. Statistics

The results were expressed as mean ± standard error of mean (SEM). One-way ANOVA with Dunnett's post-test was used to explore the significant differences between the control and other groups. $P < 0.05$ was considered significant.

3. Results

3.1. Andrographolide reverses elevation of serum transaminase in NASH mice

As shown in Table 1, the concentration of alanine/aspartate aminotransferase (ALT/AST) in serum of MCD-induced NASH mice were significantly increased compared to those in control group ($P < 0.01$), suggesting that hepatocytes were damaged. Compared with NASH model group, pioglitazone and andrographolide treatments could reverse MCD-induced liver injury by diminishing ALT and AST ($P < 0.01$).

Table 1
Effects of andrographolide on serum transaminases (means ± SEM, $n = 10$).

Groups	Doses /(mg·kg^{-1})	ALT /(U·L^{-1})	AST/ (U·L^{-1})
Control	–	13.22 ± 4.13	8.98 ± 0.83
MCD	–	177.41 ± 19.34**	33.36 ± 2.17**
Pioglitazone	10	61.67 ± 39.30$^{\#\#}$	12.07 ± 1.05$^{\#\#}$
Andrographolide	40	137.31 ± 9.15**	24.17 ± 3.36$^{**\#\#}$
Andrographolide	80	107.63 ± 24.37$^{**\#\#}$	22.40 ± 2.14$^{**\#\#}$

Note: $^{**}P < 0.01$ *vs* Control, $^{\#\#}P < 0.01$ *vs* MCD.

3.2. Effect of andrographolide on liver pathological changes in NASH mice

The tissue sections of the liver were stained with hematoxylin and eosin (H&E), and the pathological changes were observed. As shown in Fig. 1, a large amount of steatosis was found in the liver of MCD induced-NASH mice (the black arrow in Fig. 1B), accompanied by lymphocytes infiltration (the red arrow in Fig. 1B). The steatosis of hepatocytes in pioglitazone group, a positive control, was significantly improved, however, there was still a small amount of lymphocyte infiltration in pioglitazone group (Fig. 1C, red arrow). Compared with MCD induced-NASH mice, hepatocyte steatosis and lymphocyte infiltration in andrographolide treated groups were well ameliorated (Fig. 1D and E).

3.3. Analysis of potential targets of andrographolide in protecting NASH

3.3.1. Targets prediction

A total of 209 andrographolide targets (Table S1) were obtained by reverse molecular docking and molecular similarity search using the Chemical-Protein Interactome (DRAR-CPI), DrugBank, STITCH and Swiss Target Prediction database after eliminating duplicates. Moreover, 579 NASH associated targets (Table S2) were collected by GeneCards and OMIM database. Finally, 38 potential targets were obtained by overlapping the two sets (Table 2).

3.3.2. Construction and analysis of protein–protein interaction (PPI) network

A total of 38 targets information was imported into the STRING database to obtain the interaction relationship between targets, then the results with a confidence score of 0.7 or higher were introduced into Cytoscape 3.6.0 software to construct PPI network. As shown in Fig. 2, the nodes in the network represent the potential targets, and the edges represent the interaction between the targets. The network was comprised of 37 nodes and 86 edges, and the average connectivity of the nodes was 4.65.

To identify the hub nodes of the PPI network, the Network Analyzer tool in Cytoscape software was used to calculate the topological parameters of the node degree, betweenness and closeness (Table 3). The median of the degree, betweenness and closeness

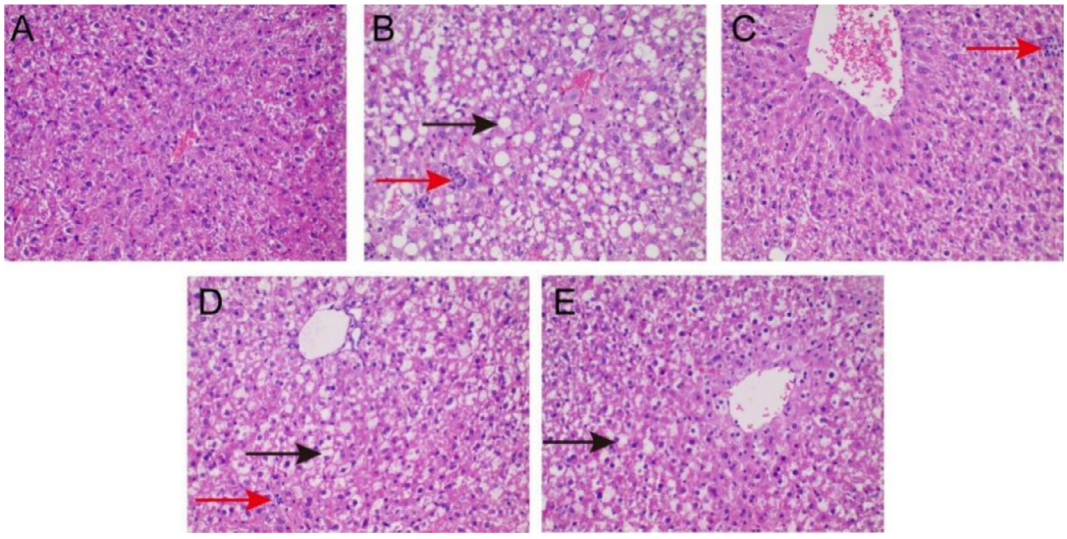

Fig. 1. Observation of histopathological changes ($n = 4$, magnification × 200). Typical images were chosen from each experimental group: (A) Control, (B) MCD, (C) Pioglitazone (10 mg/kg), (D) Andrographolide (40 mg/kg) and (E) Andrographolide (80 mg/kg). The red arrow indicates inflammatory cells infiltration, and the black arrow indicates cells steatosis.

Table 2
Putative targets of andrographolide against NASH.

No.	Gene symbols	Protein names
1	ACE	Angiotensin-converting enzyme
2	ADH1A	Alcohol dehydrogenase 1A
3	ADH1C	Alcohol dehydrogenase 1C
4	AKT1	RAC-alpha serine/threonine-protein kinase
5	CASP7	Caspase-7
6	CBS	Cystathionine beta-synthase
7	CD44	CD44 antigen
8	CETP	Cholesteryl ester transfer protein
9	CHRNA4	Neuronal acetylcholine receptor protein alpha-4 subunit
10	CTSD	Cathepsin D
11	DHFR	Dihydrofolate reductase
12	DPP4	Dipeptidyl peptidase IV
13	ELANE	Leukocyte elastase
14	ERN1	Serine/threonine-protein kinase/endoribonuclease IRE1
15	F2	Prothrombin
16	FABP1	Fatty acid-binding protein, liver (by homology)
17	FABP4	Fatty acid-binding protein, adipocyte
18	GSTM1	Glutathione S-transferase Mu 1
19	GSTP1	Glutathione S-transferase P
20	HSD11B1	Corticosteroid 11-beta-dehydrogenase isozyme 1
21	ICAM1	Intercellular adhesion molecule (ICAM-1)
22	IGF1R	Insulin-like growth factor 1 receptor
23	IL10	Interleukin-10
24	IL1B	Interleukin-1 beta
25	IL6	Interleukin-6
26	INS	Insulin
27	MAPK8	c-Jun N-terminal kinase 1
28	MAPK9	c-Jun N-terminal kinase 2
29	NR1I2	Nuclear receptor subfamily 1 group I member 2
30	NR1I3	Nuclear receptor subfamily 1 group I member 3
31	PON1	Serum paraoxonase/arylesterase 1
32	PRKCD	Protein kinase C delta
33	S100A9	Protein S100-A9
34	SERPINA1	Alpha-1-antitrypsin
35	SOD1	Superoxide dismutase [Cu-Zn]
36	SULT2A1	Bile salt sulfotransferase
37	TNF	Tumor necrosis factor
38	TTR	Transthyretin

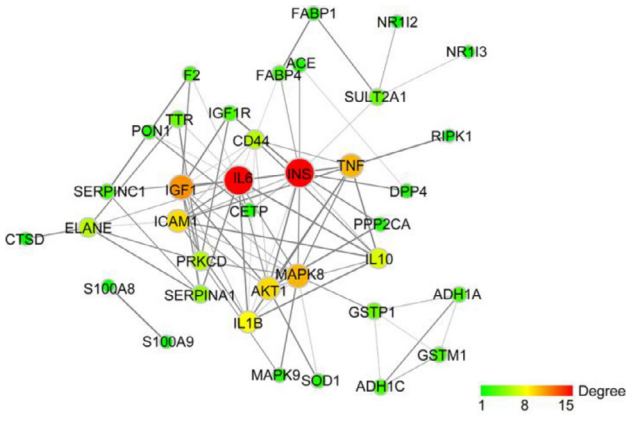

Fig. 2. Network of potential targets of andrographolide treatment for NASH analyzed by STRING. The node size and color represented the connectivity degree, and thickness of the edges represented the combine score between targets.

in the network were 3, 0.00283932 and 0.4 respectively. The nodes, with greater than 2 times of degree median and greater than the median of the other two parameters, were considered as the core targets. Thus, INS, IL6, IGF1, MAPK8, TNF, ICAM1, AKT1, IL1B and IL10 were retrieved as the most essential targets.

Table 3
Topological parameters of targets.

No.	Targets	Degree	Betweenness	Closeness
1	INS	15	0.39023852	0.59649123
2	IL6	15	0.25451575	0.5862069
3	IGF1	11	0.0796749	0.53125
4	MAPK8	10	0.28870003	0.5483871
5	TNF	10	0.07002023	0.52307692
6	ICAM1	9	0.04435461	0.52307692
7	AKT1	9	0.04200054	0.47887324
8	IL1B	8	0.00920196	0.50746269
9	IL10	7	0.0039435	0.45945946
10	ELANE	6	0.06465354	0.41975309
11	PRKCD	6	0.0326571	0.41975309
12	CD44	6	0.00092522	0.4
13	SERPINA1	5	0.00658546	0.40963855
14	SULT2A1	4	0.13065954	0.4047619
15	TTR	4	0.00283932	0.4047619
16	GSTP1	4	0.1657754	0.38202247
17	FABP4	3	0.03868093	0.425
18	IGF1R	3	0.00533486	0.425
19	F2	3	0.00148544	0.39534884
20	SERPINC1	3	0.00059418	0.38202247
21	ADH1C	3	0	0.28333333
22	ADH1A	3	0	0.28333333
23	GSTM1	3	0	0.28333333
24	PPP2CA	2	0	0.3908046
25	CETP	2	0.00653595	0.38636364
26	PON1	2	0.00505051	0.38202247
27	DPP4	2	0	0.38202247
28	ACE	2	0	0.38202247
29	SOD1	2	0.00174009	0.37777778
30	MAPK9	2	0	0.37777778
31	FABP1	2	0.0026738	0.31775701
32	S100A9	1	0	1
33	S100A8	1	0	1
34	RIPK1	1	0	0.34693878
35	CTSD	1	0	0.29824561
36	NR1I2	1	0	0.29059829
37	NR1I3	1	0	0.29059829

3.3.3. Results of GO and KEGG pathway enrichment analysis

To further analyze the molecular mechanism of andrographolide on NASH, 38 targets were submitted to g:Profiler database to perform GO and KEGG pathway enrichment, and the GO terms and KEGG pathways with P-value < 0.05 were significantly enriched (Table S3). The top 20 biological process GO terms, 15 cellular components and 17 molecular function GO terms were shown in Fig. 3A.

The KEGG pathway enrichment analysis indicated that 25 of the 38 targets (65.78%) were enriched in 43 pathways (Table S3), among which the top 20 pathways were shown in Fig. 3B. Afterwards, the 43 pathways were annotated by KEGG database (Fig. 3C). Four pathways (including AGE-RAGE signaling pathway in diabetic complications, non-alcoholic fatty liver disease (NAFLD), insulin resistance, and Type II diabetes mellitus) were classified as endocrine and metabolic disease, and three pathways (such as Inflammatory bowel disease (IBD), Graft-versus-host disease and rheumatoid arthritis) were classified as immune disease. Furthermore, there are six proteins involved in the top 20 pathways more than 10 times, including TNF (16), MAPK8 (15), IL6 (15), MAPK9(15), IL1B (14) and AKT1 (13), which suggested these targets may be the key proteins in the enriched pathways (Fig. 4).

3.3.4. Docking analysis

The targets selected for molecular docking with andrographolide were shown in Table 4, which were the pivotal targets overlapped in both PPI network and KEGG pathways. The interaction of andrographolide and the key targets were shown in Fig. 5. The results shown in Fig. 5A indicated that andrographolide bind to TNF by generating a hydrophobic interaction with the surround-

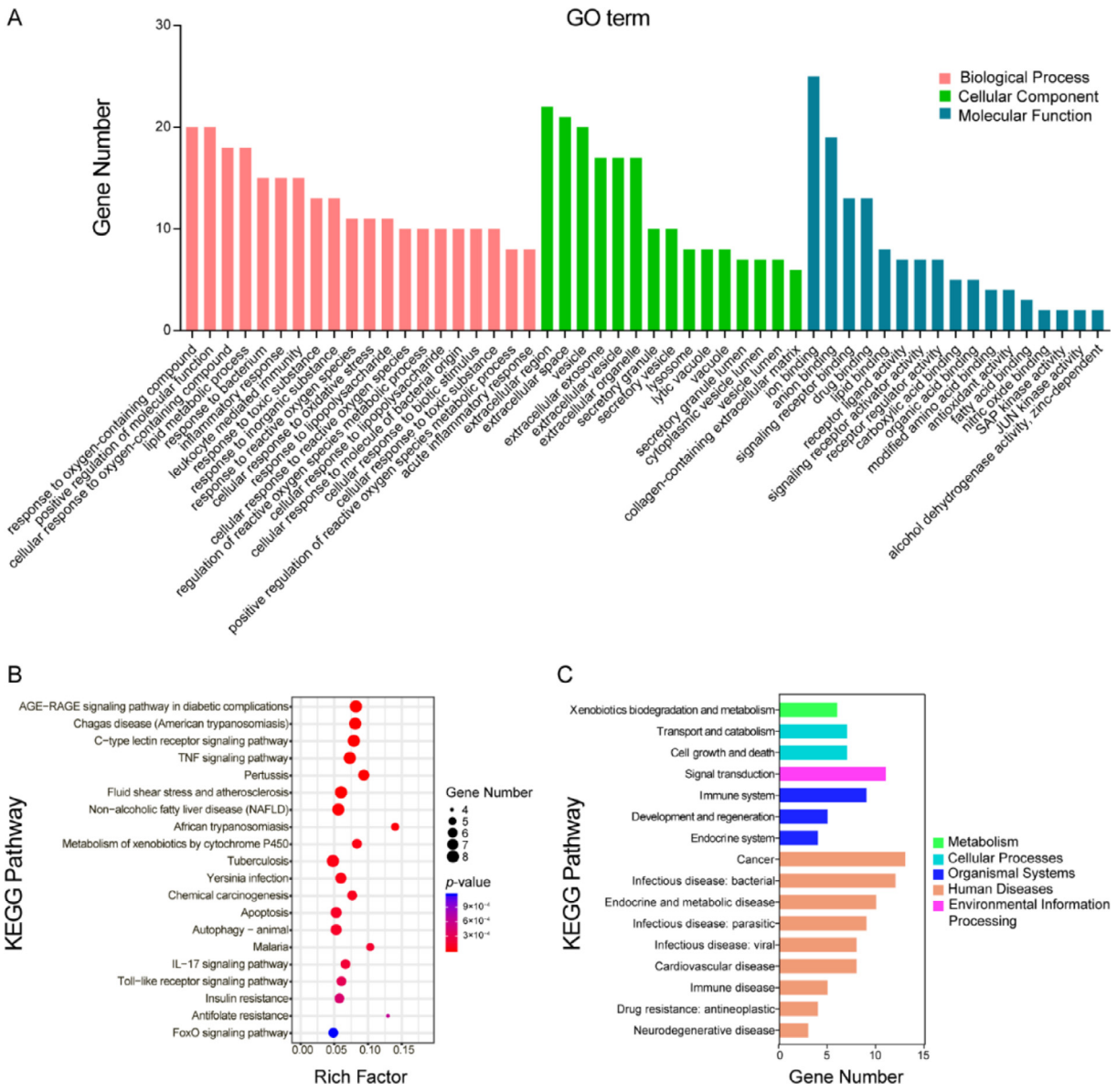

Fig. 3. GO and KEGG enrichment analysis. (A) GO enrichment of andrographolide targets; (B) KEGG pathway enrichment; (C) KEGG pathway annotation.

ing residues, including Leu55(B), Leu120(C), Tyr59(D), Ser60(D), Leu94(D), Tyr119(D) and Leu120(D). Furthermore, five hydrogen bond contacts were formed between andrographolide and $Tyr151_O$(D) (2.66 Å), $Gly121_N$(C) (3.00 Å), $Gly121_O$(C) (3.14 Å), $Gly121_N$(D) (2.65 Å) and $Gly125_N$(B) (2.75 Å), which enhanced the interaction between andrographolide and TNF. Moreover, andrographolide and MAPK8 formed five hydrophobic interaction and five H-bonds (Fig. 5B), which were at residues Ile147, Asp339, Lys340, Leu342 and Asp343 for hydrophobic interactions and $Gly146_O$ (2.762 Å), $Arg72_N$ (3.28 Å), $Ile337_N$ (3.29 Å), $Ala145_O$ (3.10 Å) and $Pro335_O$ (3.34 Å) for H-bonds. There were seven hydrophobic interactions (at the residues Leu92, Val96, Lys120, Ile123, Thr138, Pro139 and Asn144) and three hydrogen bonds ($Andrographolide_{O1}$:$Glu99_O$ (2.84 Å), $Andrographolide_{O2}$:$Glu99_O$ (2.69 Å) and $Andrographolide_{O5}$:$Glu95_O$ (2.61 Å)), shown in Fig. 5C, which illustrated the combination of andrographolide and IL6. Likewise, andrographolide can bind to IL1B by forming a hydrophobic interaction with the residues, Val19, Glu37, Gln38, Gln39, Val40, Leu62, Lys63 and Lys65, for enhancing the binding capacity, four more H-bonds were formed (Fig. 5D), $Met20_N$ (2.79 Å), $Val41_N$ (2.89 Å), $Val41_O$ (2.79 Å) and $Val41_O$ (3.08 Å). In addition, the andrographolide was predicted to interact with AKT1 by Leu156, Gly157, Lys158, Val164, Lys179, Gly233, Phe237, Glu278, Met281, Phe438 and Phe442, also four H-bonds, $Glu234_N$ (2.94 Å), $Thr291_O$ (2.71 Å), $Tyr437_O$ (2.81 Å) and $Asp439_N$ (2.79 Å), were emerged to reinforce the binding capability (Fig. 5E).

4. Discussion

As the most prevalent chronic liver disease, NAFLD imposes a huge financial burden on the social medical system. Although there is bloomed development for NAFLD associated agents during the past decade, unfortunately, there are no drugs approved for NAFLD treatment to date (Elhence & Shalimar, 2020; Friedman et al., 2018). In the absence of a proven effective therapy agents, only weight loss by bariatric surgery treatment or dietary and lifestyle modifications can be effective. However, surgery is always accom-

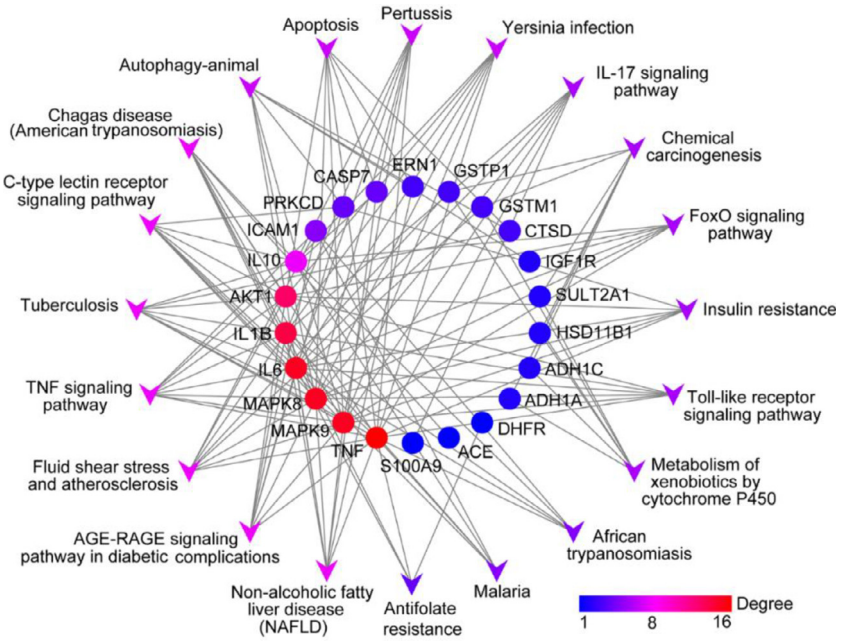

Fig. 4. Target-pathway network.

Table 4
Results of molecular docking between andrographolide and predicted targets.

Targets	PDB ID	Binding energy (ΔG)/ (kcal·mol^{-1})	Inhibit constant (Ki)/ (μmol·L^{-1})
TNF	2AZ5	−8.21	0.96
MAPK8	3PZE	−7.27	4.72
IL6	1ALU	−6.63	13.82
IL1B	6Y8M	−6.79	10.51
AKT1	4EKL	−8.90	0.30

panied by pain and injuries, and healthy lifestyle and physical training cannot be maintained for a long time, the worse is these therapies have little effect in treating NASH, a more aggressive form of NALFD. According to the Europe practice guideline (2016), the NASH patients with fibrosis stage 2 or higher should be given pharmacotherapies (Sumida & Yoneda, 2018), therefore, there is an urgent need to develop pharmacotherapies for clinical application. Numerous clinical trials showed traditional herb medicines, as complementary and alternative medicine, was widely used for treating chronic liver disease (Yan et al., 2020). Thus, it is a feasible strategy to discover candidates from traditional herb medicines for treatment of NASH.

Andrographolide is widely used to therapy for inhibiting inflammation and anti-virus in clinic. In the present study, we found that andrographolide could reduce MCD-induced liver steatosis and inflammation in mice. The mechanisms of andrographolide on amelioration of hepatic steatosis and inflammation were explored by network pharmacology-based approach. The results indicated that 38 out of 209 targets of andrographolide were involved in therapy NASH, and these targets enriched in 43 KEGG pathways. Among these proteins, IL6, TNF, INS, MAPK8 (JNK1), IRE1A, JUN (c-Jun), IL1B and CASP7 are enriched in NAFLD signaling pathway (Fig. 6).

At present, the pathogenesis of NASH has not been fully elucidated, however it is believed that NASH begins with enhanced deposition of triglycerides (TG) in the hepatocytes. Dysregulation of metabolism leading to redundant fat accumulated in the liver. Generally, the excessive fat comes from increased dietary fat intake, raised influx of free fatty acid and insulin resistance enhanced *de novo* hepatic lipogenesis. If the accumulated TG cannot be transferred by the very low density lipoprotein (VLDL) from liver or used in other metabolic pathways, the TG and free fatty acids will be deposited in hepatocytes (Oseini & Sanyal, 2017). In the present study, the predicted targets of andrographolide, IL6 (enriched in type Ⅱ diabetes bellitus), TNF (involved in TNF signaling pathway), INS and AKT (connected with insulin and PI3K/AKT signaling pathway), were participate in regulation of *de novo* fatty acid biosynthesis and associated with insulin resistance, which can lead to hepatic steatosis. In addition, Ding found that andrographolide could inhibit the transcriptional activity of SREBPs (Ding et al., 2014), which also regulate *de novo* fatty acids synthesis. These findings further elucidate the regulation of andrographolide on *de novo* fatty acids synthesis.

Although TG is not considered as a hepatotoxic, the fatty acids, involved in TG metabolism and synthesis, is thought to be the hepatocyte lipotoxicity within the liver and results in mitochondria and endoplasmic reticulum stress to release of reactive oxygen species (ROS) and recruitment of immune cells and associated mediators (Neuschwander-Tetri, 2010). Then, further hepatocyte injuries were occurred by oxidative stress, inflammation, and apoptosis (Oseini & Sanyal, 2017). The result of KEGG enrichment analysis showed the predicted targets of andrographolide, including TNF, JNK1, JUN, IRE1A, IL1B and IL6, were involved in the development of steatohepatitis. Moreover, TNF also induces hepatocyte death and inflammation. Numerous studies revealed that the anti-inflammatory effects of andrographolide were mediated by regulating TNF, JNK, JUN, IL1B, IL6 (Li et al., 2017; Sechet et al., 2018), and andrographolide can directly or indirectly inhibit oxidative stress by protecting mitochondria or suppressing the specific ROS-producing enzymes to prevent free-radical formation, and activating Nrf2 signaling pathway to activate enzymatic or non-enzymatic anti-oxidants (Mussard et al., 2019). These studies suggested anti-inflammatory and anti-oxidative effects of andrographolide may play a critical role in amelioration of NASH.

To replace the dying hepatocyte, the complexed wound healing is launched to restore the liver structure and function. However,

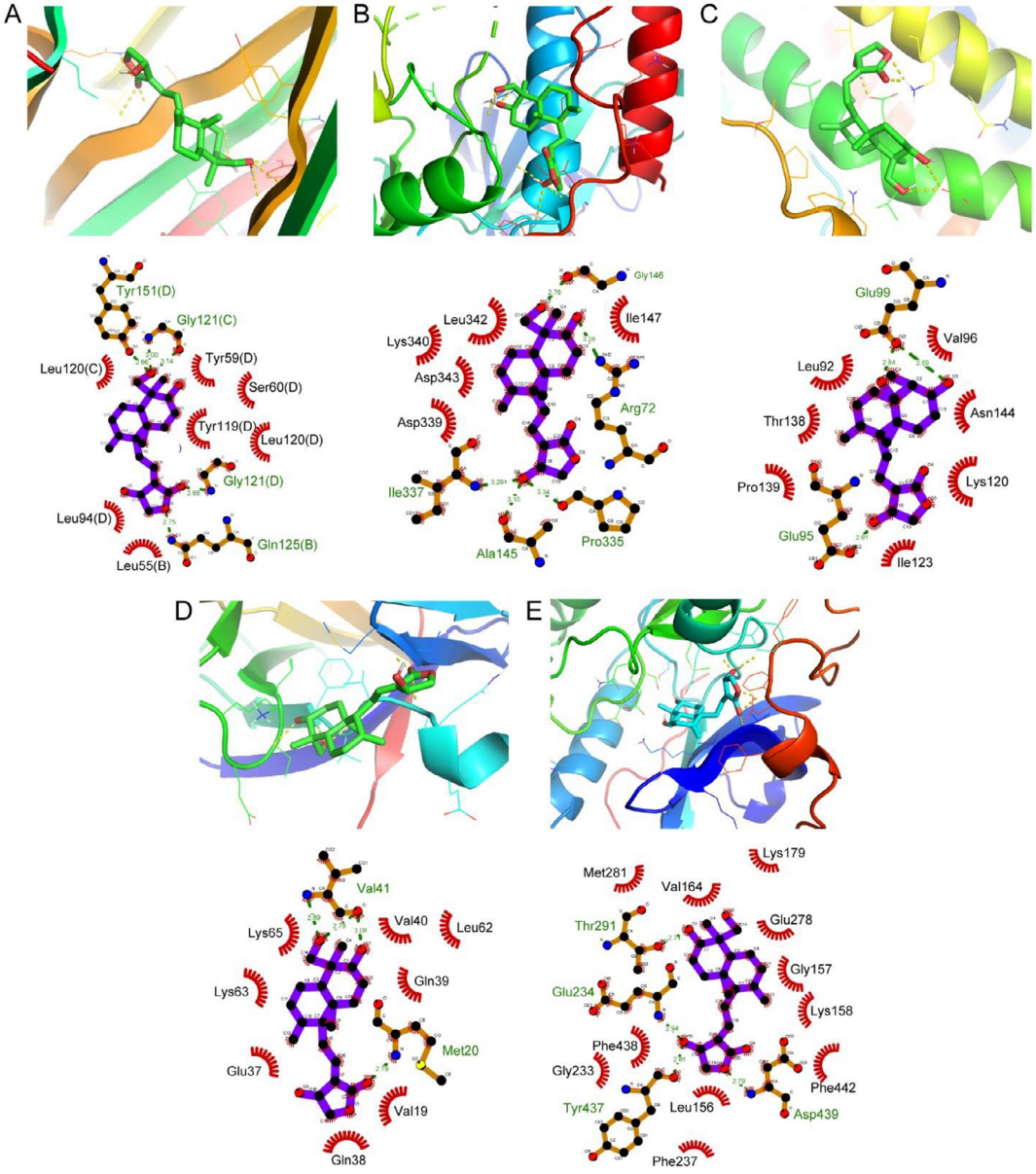

Fig. 5. 3D and 2D diagrams of molecular models of andrographolide with predicted targets of TNF (A), MAPK8 (B), IL6 (C), IL1B (D) and AKT1 (E).

aberrations in wound healing process can lead to defective or dysregulated restore of the injured hepatocytes and cause cirrhosis or HCC (MacHado & Diehl, 2016). Cabrera *et al.* found andrographolide could ameliorate inflammation and fibrogenesis by attenuating inflammasome activation in experimental NASH (Cabrera et al., 2017). Furthermore, it was found andrographolide could activate Nrf2-mediated anti-oxidative signaling pathway to improve acetaminophen-induced liver fibrosis (Yan et al., 2018). Although there are no targets related with anti-fibrosis predicted by the network pharmacology, the previous findings suggested anti-fibrogenesis may contribute against NASH for andrographolide.

To confirm the reliability of the predicted targets of andrographolide, molecular docking was performed. The results showed andrographolide could interactive with the selected hub targets, which suggested the correctness of our research at least in theory. However, the mechanisms of andrographolide ameliorating NASH still need to be further verified by *in vivo* and/or *in vitro* studies.

5. Conclusion

Taking together, the bioinformatics approach by network pharmacology revealed the potential targets in regulating *de novo* fatty acids synthesis, anti-inflammation and anti-oxidation contribute to the improvement of NASH by andrographolide. Moreover, the anti-fibrotic effect of andrographolide may also play a role. The results indicated "multiple targets, multiple pathways" 1mechanisms of the traditional Chinses medicine in treatments of chronic diseases.

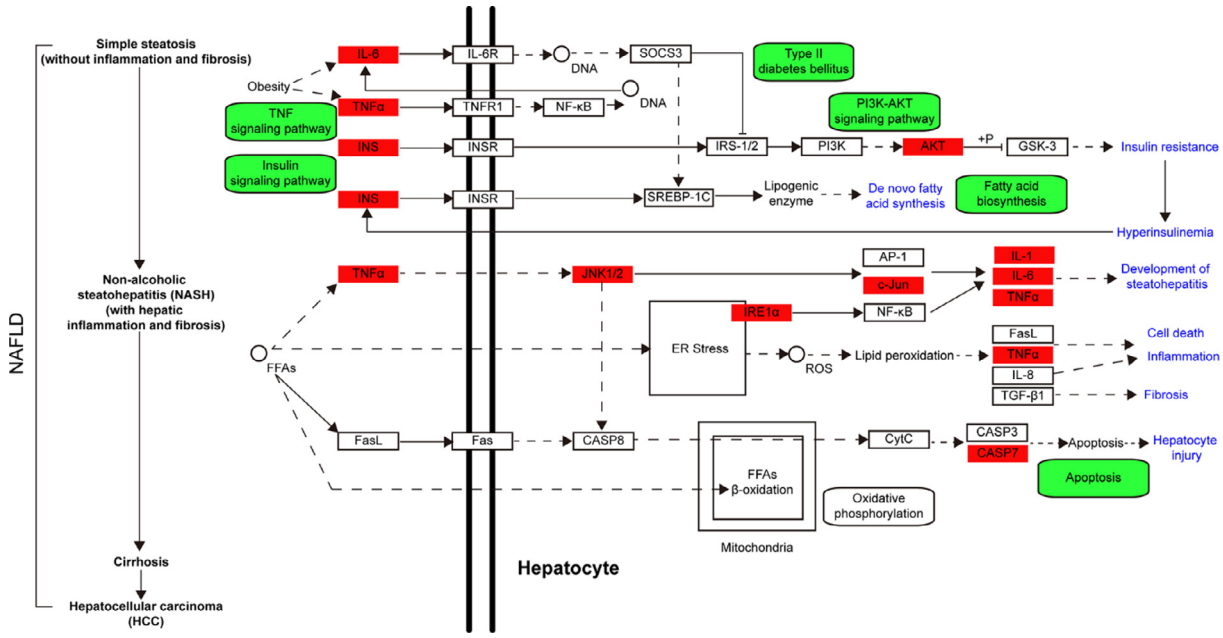

Fig. 6. Mechanisms of andrographolide against NASH.

Declaration of Competing Interest

The authors declare that they have no known competing financial interests or personal relationships that could have appeared to influence the work reported in this paper.

Acknowledgements

This research was funded by the National Natural Science Foundation of China (31802242), Young Talents Visiting and Training Program for Foreign Country of Anhui Education Department (gxgwfx2019047), the National Natural Science Foundation of Anhui (2008085QC146), Natural Science Key Foundation of Anhui Education Department (KJ2017A503, KJ2017A504), Talent Project of Anhui Science and Technology University (ZRC2014447), and Key Research and Development Plan of Anhui Province (202004a06020050). Also, the authors would like to thank Dr. Ruth Wonfor, the Institute of Biological, Environmental and Rural Sciences (IBERS), Aberystwyth University, UK, for her good suggestion and language edit.

Appendix A. Supplementary data

Supplementary data to this article can be found online at https://doi.org/10.1016/j.chmed.2021.05.001.

References

Bedogni, G., Nobili, V., & Tiribelli, C. (2014). Epidemiology of fatty liver: An update. *World Journal of Gastroenterology, 27*, 9050–9054.

Cabrera, D., Wree, A., Povero, D., Solís, N., Hernandez, A., Pizarro, M., ... Arrese, M. (2017). Andrographolide ameliorates inflammation and fibrogenesis and attenuates inflammasome activation in experimental non-alcoholic steatohepatitis. *Scientific Reports, 7*(1), 1–12.

Chen, H. W., Huang, C. S., Li, C. C., Lin, A. H., Huang, Y. J., Wang, T. S., ... Lii, C. K. (2014). Bioavailability of andrographolide and protection against carbon tetrachloride-induced oxidative damage in rats. *Toxicology and Applied Pharmacology, 280*(1), 1–9.

Daina, A., Michielin, O., & Zoete, V. (2019). SwissTargetPrediction: Updated data and new features for efficient prediction of protein targets of small molecules. *Nucleic Acids Research, 47*, 357–364.

Das, S., Pradhan, G. K., Das, S., Nath, D., das, K., & Saha (2015). Enhanced protective activity of nano formulated andrographolide against arsenic induced liver damage. *Chemico-Biological Interactions, 242*, 281–289.

Ding, L., Li, J., Song, B., Xiao, X., Huang, W., Zhang, B., ... Wang, Z. (2014). Andrographolide prevents high-fat diet-induced obesity in C57BL/6 mice by suppressing the sterol regulatory element-binding protein pathway. *Journal of Pharmacology and Experimental Therapeutics, 351*(2), 474–483.

Elhence, A., & Shalimar. (2020). Treatment of non-alcoholic fatty liver disease — Current perspectives. *Indian Journal of Gastroenterology, 39*(1), 22–31.

Fazel, Y., Koenig, A. B., Sayiner, M., Goodman, Z. D., & Younossi, Z. M. (2016). Epidemiology and natural history of non-alcoholic fatty liver disease. *Metabolism: Clinical and Experimental, 65*(8), 1017–1025.

Friedman, S. L., Neuschwander-Tetri, B. A., Rinella, M., & Sanyal, A. J. (2018). Treatment of non-alcoholic fatty liver disease — Current perspectives. *Nature Medicine, 24*(7), 908–922.

Hamosh, A., Scott, A. F., Amberger, J. S., Bocchini, C. A., & Mckusick, V. A. (2005). Online Mendelian Inheritance in Man (OMIM), a knowledgebase of human genes and genetic disorders. *Nucleic Acids Research, 33*, 514–517.

Hossain, Md. S., Urbi, Z., Sule, A., & Rahman, K. M. H. (2014). Andrographis paniculata (Burm. f.) Wall. ex Nees: A review of ethnobotany, phytochemistry, and pharmacology. *The Scientific World Journal*, 2014, 274905.

Ji, L., Liu, T., Liu, J., Chen, Y., & Wang, Z. (2007). Andrographolide inhibits human hepatoma-derived Hep3B cell growth through the activation of c-Jun N-terminal kinase. *Planta Medica, 73*(13), 1397–1401.

Ji, X., Li, C., Ou, Y., Li, N., Yuan, K., Yang, G., ... Lan, T. (2016). Andrographolide ameliorates diabetic nephropathy by attenuating hyperglycemia-mediated renal oxidative stress and inflammation via Akt/NF-κB pathway. *Molecular and Cellular Endocrinology, 437*, 268–279.

Li, Y., He, S., Tang, J., Ding, N., Chu, X., Cheng, L., Ding, X., Liang, T., Feng, S., Rahman, S. U., Wang, X., & Wu, J. (2017). Andrographolide inhibits inflammatory cytokines secretion in LPS-stimulated RAW264.7 cells through suppression of NF-κB/MAPK signaling pathway. *Evidence-Based Complementary and Alternative Medicine*, 2017, 8248142-undefined.

Luo, H., Chen, J., Shi, L., Mikailov, M., Zhu, H., Wang, K., ... Yang, L. (2011). DRAR-CPI: A server for identifying drug repositioning potential and adverse drug reactions via the chemical-protein interactome. *Nucleic Acids Research, 39*, 492–498.

MacHado, M. V., & Diehl, A. M. (2016). Pathogenesis of nonalcoholic steatohepatitis. *Gastroenterology, 150*(8), 1769–1777.

Miao, X., Zheng, L., Zhao, Z., Su, S., Zhu, Y., Guo, J., ... Duan, J. (2019). Protective effect and mechanism of boswellic acid and myrrha sesquiterpenes with different proportions of compatibility on neuroinflammation by LPS-induced BV2 cells combined with network pharmacology. *Molecules, 24*(21), 3946.

Mittal, S. P. K., Khole, S., Jagadish, N., Ghosh, D., Gadgil, V., Sinkar, V., & Ghaskadbi, S. S. (2016). Andrographolide protects liver cells from H_2O_2 induced cell death by upregulation of Nrf-2/HO-1 mediated via adenosine A2a receptor signalling. *Biochimica et Biophysica Acta - General Subjects, 1860*(11), 2377–2390.

Morris, G. M., Ruth, H., Lindstrom, W., Sanner, M. F., Belew, R. K., Goodsell, D. S., & Olson, A. J. (2009). Software news and updates AutoDock4 and AutoDockTools4: Automated docking with selective receptor flexibility. *Journal of Computational Chemistry, 30*(16), 2785–2791.

Mussard, E., Cesaro, A., Lespessailles, E., Legrain, B., Berteina-Raboin, S., & Toumi, H. (2019). Andrographolide, a natural antioxidant: An update. *Antioxidants, 8*(12), 571.

Neuschwander-Tetri, B. A. (2010). Hepatic lipotoxicity and the pathogenesis of nonalcoholic steatohepatitis: The central role of nontriglyceride fatty acid metabolites. *Hepatology, 52*(2), 774–788.

Oseini, A. M., & Sanyal, A. J. (2017). Therapies in non-alcoholic steatohepatitis (NASH). *Liver International, 37*, 97–103.

Qian, K., Liu, Y. Y., Zhang, Y., Chen, Y., & Wu, W. H. (2020). Research progress on molecular mechanism of traditional Chinese medicine against non-alcoholic fatty liver disease. *Chinese Traditional and Herbal Drugs, 51*(19), 5083–5092.

Raudvere, U., Kolberg, L., Kuzmin, I., Arak, T., Adler, P., Peterson, H., & Vilo, J. (2019). g:Profiler: A web server for functional enrichment analysis and conversions of gene lists (2019 update). *Nucleic Acids Research, 47*, 191–198.

Rocha, A. L., Oliveira, F. R., Azevedo, R. C., Silva, V. A., Peres, T. M., Candido, A. L., ... Reis, F. M. (2019). Treatment of non-alcoholic fatty liver disease — Current perspectives. *F1000Research, 8*, 565.

Rosmorduc, O., & Fartoux, L. (2012). Treatment of non-alcoholic fatty liver disease — Current perspectives. *Clinics and Research in Hepatology and Gastroenterology, 36*(3), 202–208.

Sechet, E., Telford, E., Bonamy, C., Sansonetti, P. J., & Sperandio, B. (2018). Natural molecules induce and synergize to boost expression of the human antimicrobial peptide β-defensin-3. *Proceedings of the National Academy of Sciences of the United States of America. The Scientific World Journal*, 115(42), E9869–E9878.

Singha, P. K., Roy, S., & Dey, S. (2007). Protective activity of andrographolide and arabinogalactan proteins from *Andrographis paniculata* Nees. against ethanol-induced toxicity in mice. *Journal of Ethnopharmacology, 111*(1), 13–21.

Stelzer, G., Rosen, N., Plaschkes, I., Zimmerman, S., Twik, M., Fishilevich, S., ... Lancet, D. (2016). The GeneCards suite: From gene data mining to disease genome sequence analyses. *Current Protocols in Bioinformatics, 2016*(1).

Sumida, Y., & Yoneda, M. (2018). Current and future pharmacological therapies for NAFLD/NASH. *Journal of Gastroenterology, 53*(3), 362–376.

Szklarczyk, D., Gable, A. L., Lyon, D., Junge, A., Wyder, S., Huerta-Cepas, J., ... von Mering, C. (2018). STRING v11: Protein-protein association networks with increased coverage, supporting functional discovery in genome-wide experimental datasets. *Nucleic Acids Research, 47*, 607–613.

Szklarczyk, D., Santos, A., von Mering, C., Jensen, L. J., & Kuhn, M. (2016). STITCH 5: Augmenting protein-chemical interaction networks with tissue and affinity data. *Nucleic Acids Research, 44*, D380–D384.

Thakur, A. K., Rai, G., Chatterjee, S. S., & Kumar, V. (2016). Beneficial effects of an Andrographis paniculata extract and andrographolide on cognitive functions in streptozotocin-induced diabetic rats. *Pharmaceutical Biology, 54*(9), 1528–1538.

Vernon, G., Baranova, A., & Younossi, Z. M. (2011). Treatment of non-alcoholic fatty liver disease — Current perspectives. *Alimentary Pharmacology and Therapeutics, 34*(3), 274–285.

Wang, X., Su, R., Guo, Q., Liu, J., Ruan, B., & Wang, G. (2019). Competing endogenous RNA (ceRNA) hypothetic model based on comprehensive analysis of long non-coding RNA expression in lung adenocarcinoma. *PeerJ, 2019*(11) e8024.

Wintachai, P., Kaur, P., Lee, R. C. H., Ramphan, S., Kuadkitkan, A., Wikan, N., ... Smith, D. R. (2015). Activity of andrographolide against chikungunya virus infection. *Scientific Reports, 5*(1), 1–14.

Wishart, D. S., Feunang, Y. D., Guo, A. C., Lo, E. J., Marcu, A., Grant, J. R., ... Wilson, M. (2018). DrugBank 5.0: A major update to the DrugBank database for 2018. *Nucleic Acids Research, 46*, D1074–D1082.

Wruck, W., Graffmann, N., Kawala, M. A., & Adjaye, J. (2017). Concise review: Current status and future directions on research related to nonalcoholic fatty liver disease. *Stem Cells, 35*(1), 89–96.

Xiao, J., Wang, F., Wong, N. K., He, J., Zhang, R., Sun, R., ... Li, C. (2019). Treatment of non-alcoholic fatty liver disease — Current perspectives. *Journal of Hepatology, 71*(1), 212–221.

Yan, H., Huang, Z., Bai, Q., Sheng, Y., Hao, Z., Wang, Z., & Ji, L. (2018). Natural product andrographolide alleviated APAP-induced liver fibrosis by activating Nrf2 antioxidant pathway. *Toxicology, 396–397*, 1–12.

Yan, T., Yan, N., Wang, P., Xia, Y., Hao, H., Wang, G., & Gonzalez, F. J. (2020). Treatment of non-alcoholic fatty liver disease — Current perspectives. *Acta Pharmaceutica Sinica B, 10*(1), 3–18.

Yu, Z., Lu, B., Sheng, Y., Zhou, L., Ji, L., & Wang, Z. (2015). Andrographolide ameliorates diabetic retinopathy by inhibiting retinal angiogenesis and inflammation. *Biochimica et Biophysica Acta - General Subjects, 1850*(4), 824–831.

Zhao, J., Yang, J., Tian, S., & Zhang, W. (2019). Treatment of non-alcoholic fatty liver disease — Current perspectives. *Quantitative Biology, 7*(1), 17–29.

Zhou, Y. J., Li, Y. Y., Nie, Y. Q., Ma, J. X., Lu, L. G., Shi, S. L., ... Hu, P. J. (2007). Prevalence of fatty liver disease and its risk factors in the population of South China. *World Journal of Gastroenterology, 13*(47), 6419–6424.